

# BLOCKAGE RATIO INFLUENCE IN 2-D BLUFF BODY NEAR WAKE AT LOW REYNOLDS NUMBER

Tiago Barbosa de Araújo, [araujotb@ita.br](mailto:araujotb@ita.br)

Roberto da Mota Girardi, [girardi@ita.br](mailto:girardi@ita.br)

Mauricio Pedrassi, [pedrassi@ita.br](mailto:pedrassi@ita.br)

Instituto Tecnológico de Aeronáutica, Praça Mal. do ar Eduardo Gomes, 50, Vila das Acácias - São José dos Campos - SP - Brazil

**Abstract.** *Despite largely studied, the flow over bluff bodies still has some features that are not clearly understood. These features, characterized by non-dimensional numbers, can be related in their midst for a better comprehension of this kind of flow. The non-dimensional numbers, such as the base pressure coefficient, drag coefficient and Strouhal number can also be correlated to near wake parameters, such as the formation region length and width. These numbers can also vary as the blockage ratio change in wind tunnel experiments, so the aim of this paper is to show how they are connected to the formation region parameters behavior of two-dimensional flow over a wedge model. However the measurement of velocities fields in the base of a bluff body is not a simple task, because of recirculation zone and the very low velocities associated to it. Then, to accomplish this task a laser Doppler anemometer is used with an experimental procedure developed to this work. With this equipment and procedure the mean ( $u$  and  $v$ ) and the fluctuant ( $u_{RMS}$  e  $v_{RMS}$ ) velocities of a wedge model base flow were acquired for two different blockage ratio at the same Reynolds number ( $3.0 \times 10^3$ ), allowing the observation of the blockage influence in the near wake.*

**Keywords:** *Bluff body, Blockage ratio, Near wake, LDA.*

## 1. Introduction

During decades a better understanding about the flow over bluff bodies have been aimed by scientists and engineers. The interesting in this kind of flow is due to its high applicability, such as in heat exchangers (Ahlborn et al, 2002), where great flow mixing occurs in the body wake providing better heat exchange, or in the building industry, where the studies focus in the aerodynamic load over bridges and buildings (Tamura et al, 2003).

Due its complexity there isn't a theory able to predict, mainly, the drag coefficient and other interesting flow parameters, such as Strouhal number ( $St$ ), base pressure coefficient ( $C_{pb}$ ) and wake width ( $d'$ ). Because of it some predictions are only possible using semi-empirical methods, such as the one developed by von Kármán for drag prediction (Williamson, 1996), or computational methods, such as Direct Numerical Simulation ( $DNS$ ).

Another way of striking this problem out is using experimental approach, which is still largely used. Such studies were conducted by Roshko (1954) and Bearman (1965), where they used splitter plates, placed in the symmetry wake flow line of two-dimensional bluff bodies, to change the wake flow. In the first paper, Roshko has used one splitter plate of fixed length, which was first placed at the body base and then moved away from there along the symmetry flow line.

In the second one, Bearman used different length splitter plates attached at the body base. In their studies these authors have shown the existence of some correlations among the flow parameters, such as drag coefficient, base pressure coefficient and Strouhal number, which could also be related to near wake characteristic lengths. An interesting observation made by Roshko in his work, moving the splitter plate, is that when the plate is placed at certain distance from the body base, the flow parameters changing ceases, returning to the original body flow, without interference. This region is known as vortex formation region.

Despite both authors have used splitter plates on the symmetry flow line, inserting an interfering element attached at different base positions also implies on flow parameters changing. Rathakrishnan (1999) used a fixed length splitter plate fixed at different positions on the body base and shown that it also varies the flow parameters, but with less intensity.

Another interfering way on the flow parameters, without inserting a physical element in the formation region is through blockage ratio variation (Araújo, 2008). The blockage ratio increasing leads to base pressure and the formation region length (near wake) decreasing, however, keeping the wake width almost unchanged (Sousa, 1993).

The series of experimental studies, related previously, show the near wake importance on bluff bodies flow understanding. Then, for better knowing this flow region and the blockage influence over it, velocity fields are acquired. However this flow region is well known as a recirculation zone, where the velocities are very low and the flow direction is constantly changing. These facts make the use of hot wire anemometer ( $HWA$ ) inappropriate, because the calibration for the velocity range becomes hard and with large uncertainties, and the  $HWA$  cannot distinguish the velocity components.

To make this measurements, a laser Doppler anemometer ( $LDA$ ) was chosen, because it is a non-intrusive method and does not need of calibration (Dantec Dynamics, 2005). Furthermore, the  $LDA$  system is also able to differentiate the flow velocity direction, making it suitable for the required measurements. In this paper will be presented near wake flow

fields to two different blockage ratio (9.8% e 19.7%) for a wedge model with  $90^\circ$  of apex angle. The mean ( $u$  and  $v$ ) and the fluctuant ( $u_{RMS}$  e  $v_{RMS}$ ) velocities fields presented here were obtained for a fixed and low Reynolds number.

## 2. Experimental Apparatus

The measurements were performed in an open circuit wind tunnel, where the fan is placed after the test section, manufactured by *TSI* (model 8390), as we can see in Fig. 1. The test section is square and characterized by the dimension of 101.6 millimeters and the contraction ratio of 4:1. This wind tunnel was chosen due to its low turbulence level and its flow quality to low velocities. The flow velocity ranges from 1.0  $m/s$  to 32.0  $m/s$  and the turbulence level is of 1.2% with the flow seeding presence, since one interest of this paper is getting reliable results at low Reynolds number using LDA.

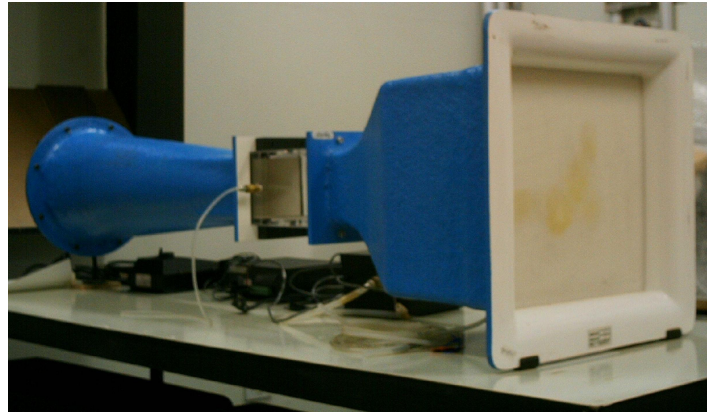


Figure 1. Wind tunnel model 8390 with square test section characterized by the dimension of 101.6  $mm$ .

The models used in this work are wedges with apex angle of  $90^\circ$  (see fig. 2) with two different blockage ratio, 9.8% e 19.7%. The aspect ratios of all models are equal to 10.2 e 5.1, which the end effects can't be neglected, but only at the mean span, where the measurements are taken. For this case parallel vortex shedding could be observed by Mittal (2001). Then, at the model central plane the flow can be considered two-dimensional.

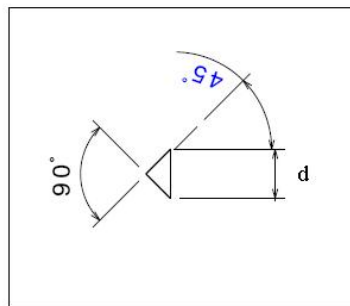


Figure 2. Wedge lateral view. The parameter  $d$  is equal to 10 $mm$  and 20 $mm$  for the blockage of 9.8% and 19.7%, respectively.

The models are placed in the test section in such a way that they stay perpendicular to the plane  $XOY$ , as shown in the Fig. 3. The axis models pass through one of tunnel window with its position placed at 90.0  $mm$  from the test section beginning and 50.8  $mm$  from the wind tunnel lower surface, fixing the model.

To perform the flow measurements was used a LDA system equipped with an Argon-Krypton laser, which produces visible light with power emission of 5.44  $W$  in its entire spectrum. From the emission spectrum three colors are selected by the optical system, which are 514.5  $nm$ , 488.0  $nm$  and 476.5  $nm$  wavelength.

This LDA is able to make three-dimensional measurements, however as the mean span flow can be considered two-dimensional, we have opted by using the 2-D configuration, which uses a two-dimensional probe fitted with the two first wavelengths. Its measurement volume was placed in central plane by adjusting the distance between the two incoming beams, and using the optics relations to know the beams deflection due to crossing by the window, which was made of acrylic (reflection index of 1.49). In the figure 4 is presented a picture of the system with its parts labeled. The LDA probe was mounted on a bench which was placed together at two-dimensional traverse with 0.1  $mm$  precision.

The measurement system is based on light reflections, where two test section incoming laser beams interfere to each other forming dark and light fringes. One seeding particle passing by these fringes will reflect back the part of the laser

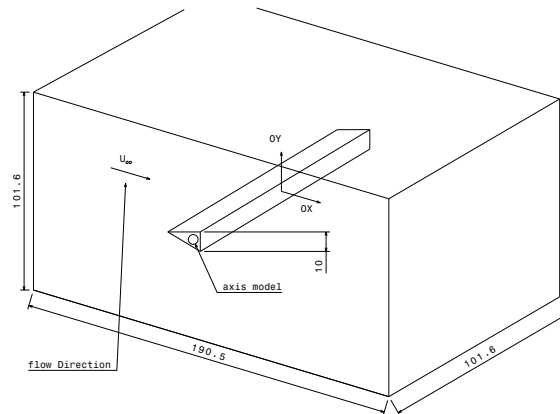


Figure 3. Test section view with a model placed at its position, with the coordinate system adopted.

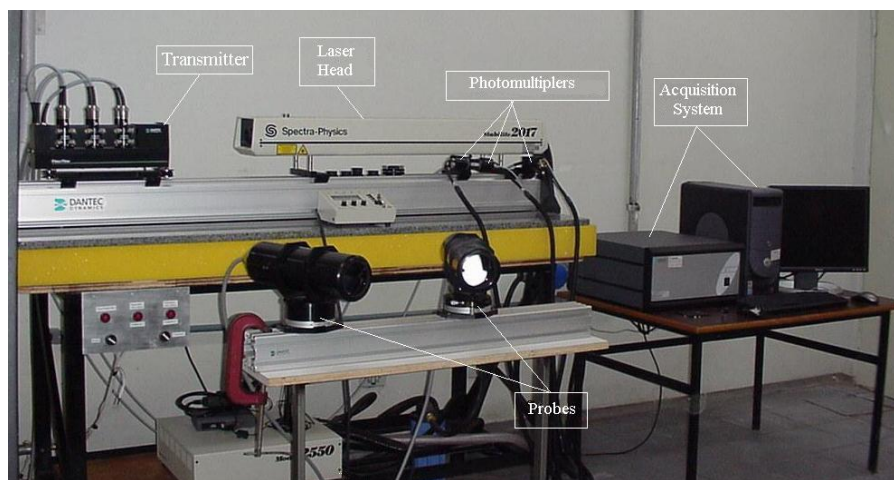


Figure 4. General view of the LDA setup.

beams from light fringes to the photomultipliers at known frequency ( $f_D$ ), which due to the particles velocity is different from the incoming laser (Doppler effect) and also different for each measured velocity. Then the distance between two light (or dark) fringes ( $\delta_f$ ) can be determined from the optics and given by:

$$\delta_f = \frac{\lambda}{2 \sin(\theta/2)} \quad (1)$$

Where  $\lambda$  and  $\theta$  are the incoming wavelength and the angle between the two incoming laser beams, consecutively. Then the velocity can be determined by the product of  $f_D$  and  $\delta_f$ , as shown in the equation (2):

$$\mathbf{u} = f_D \cdot \delta_f = \frac{\lambda}{2 \sin(\theta/2)} \cdot f_D \quad (2)$$

The flow seeding used in this work were olive oil, which was atomized in particle generator made by TSI (model 9307). This generator was calibrated to produce droplets with mean diameter of  $1.0 \mu m$ , which are suitable for low Mach number regimes and for turbulent flow with  $10 \text{ KHz}$  maximum frequency (Melling, 1997). The dynamic pressure was controlled by a WIKA (Tronic Line) micromanometer which ranges from  $0.0 \text{ mbar}$  to  $1.0 \text{ mbar}$  ( $100,0 \text{ Pa}$ ). This was calibrated from  $0.0 \text{ m/s}$  to  $12.0 \text{ m/s}$ .

### 3. Experimental Procedure

Considering the model set in the wind tunnel section as shown in the figure 3 and its is aligned with the flow direction (see Araújo and Girardi, 2009), other two problems must be taken in account for getting reliable measurements. First is the measurement time, which must be different inside and outside the wake, which are 64 and 32 seconds, consecutively (see Araújo and Girardi, 2008), with particle density larger than 100 particles per second. The different times are due to flow characteristics in each region. Inside the wake the flow oscillates because of the vortex passage, which makes the acquiring time necessary to confident mean larger than outside, where the flow oscillations are attenuated. Second is the LDA system alignment, what is described below.

With the traverse and wind tunnel coordinated systems aligned to each other, we have to ensure that the measurement volume is at the model mead-span. Once the incoming laser beams have to pass through the wind tunnel window, it is necessary to calculate measurement volume displacement. Knowing the window refraction index is easy to calculate, using geometric optics, the measurement volume displacement due to window presence as a function of its width. Then, we can calculate the distance between two beams, of the same color and probe, at the window incoming surface, which is 4.65 millimeters to our setup.

After crossing the wind tunnel test section the laser beam reaches a wall, black painted, where there are two marks at middle high, one at the section beginning and the other at its end, as we can see schematically at the figure 5. The marks are represented by the points A and B. If we move the probe along a straight line beginning at the point A and finishing at the point B, it means that the alignment in the plane  $XOY$  is done.

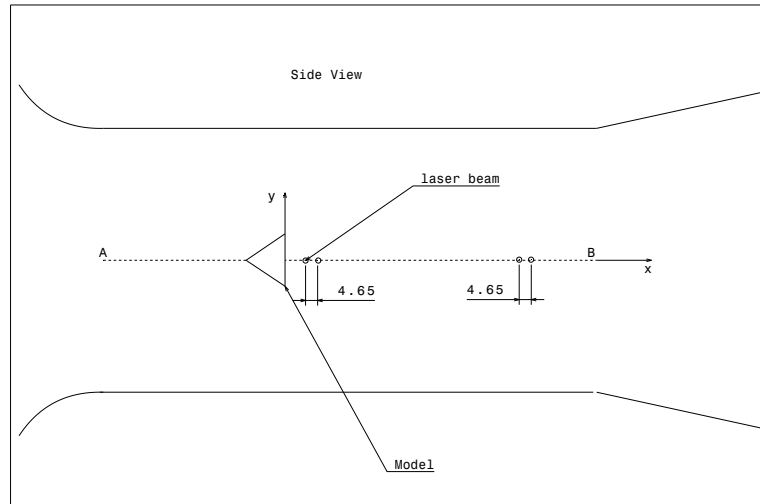


Figure 5. Test section side view with the two marks used during the alignment.

To the alignment in the plane  $XOZ$  we just have to ensure that, while the laser probe is moving, the distance between the two laser beams is kept constant along the line, at the window incoming surface, as we can see schematically in the figure 6. When it is achieved we can consider the alignment in the plane  $XOZ$  done.

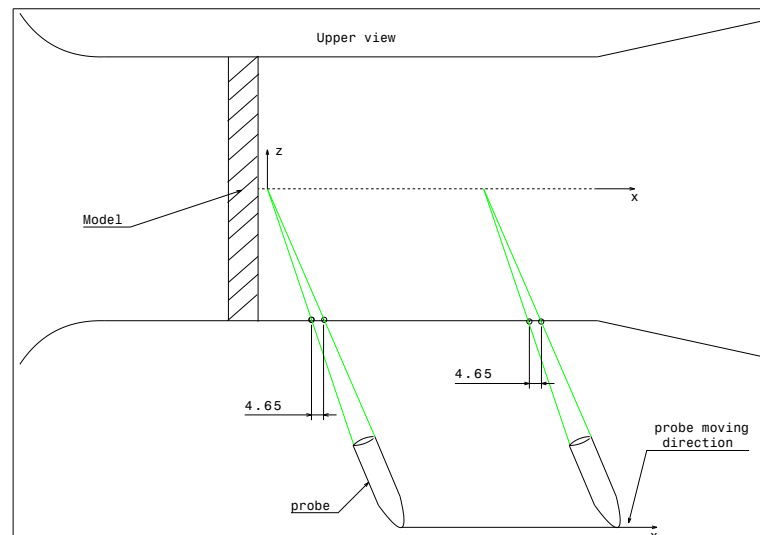


Figure 6. Test section upper view showing the  $XOZ$  alignment.

With the laser probe and test section aligned to each other, the measurement volume is placed at the system origin (see figure 3), which is located at middle-span and at the base center ( $0.5d$ ) and the velocity profiles can be taken. From there the measurement volume is placed at  $-0.2d$  in the  $y$ -direction and is moved until the position  $1.2d$  by increments of  $0.1d$ , except near the separation point where the increments are refined to  $0.05d$ . This procedure takes one velocity profile at the  $y$ -direction and it is repeated along the  $x$ -direction until  $x = 3.0d$ , by increments of  $0.1d$  from the body base to  $x = 2.0d$

and by increments of  $0.2d$  from there to  $x = 3.0d$ .

#### 4. Results

This section will be pointed out the flow changing characteristics due to the blockage ratio variation, keeping the Reynolds number constant and equal to  $3.0 \times 10^3$  and all the uncertainty shown are with probability of 95%. The model angle of attack for both experiments are equal to zero. Using the Laser Doppler anemometry advantage over the hot wire anemometry is possible to obtain the vorticity, defined by equation (3), field experimentally. It is also used the finite difference to obtain the velocities derivatives.

$$\omega_z = \frac{1}{2} \left( \frac{\partial v}{\partial x} - \frac{\partial u}{\partial y} \right) \quad (3)$$

In the figure 7 are shown the mean vorticity field on its non-dimensional form ( $\frac{\omega_z d}{U_\infty}$ ), for both blockage ratios. The points N and S are the mean vortex core position and saddle point, respectively. The high uncertainties obtained for the vorticity fields using the finite difference method, are due to traverse low precision ( $0.1mm$ ).

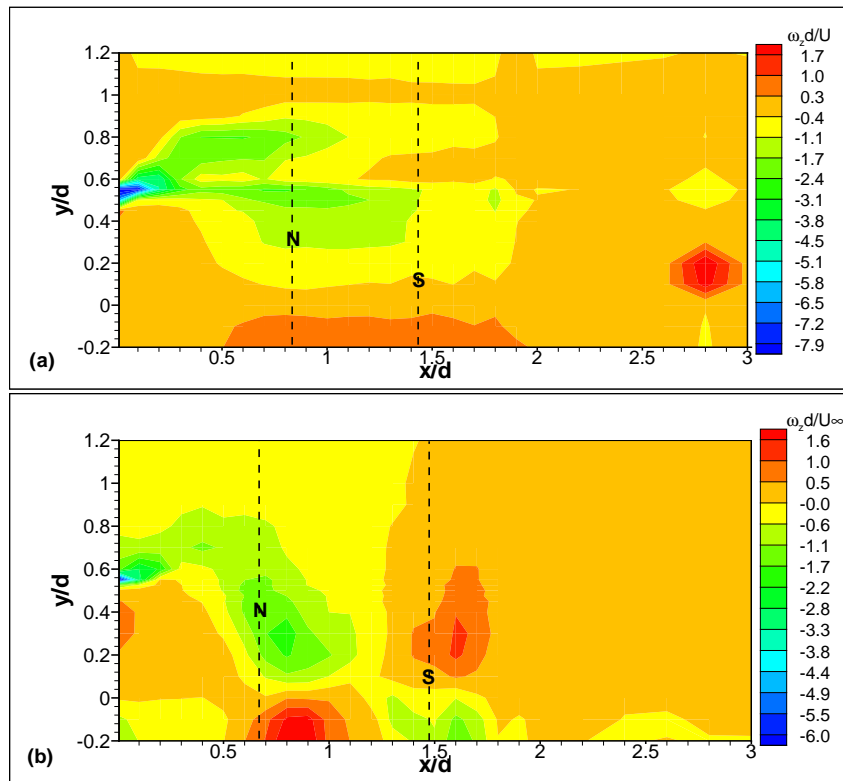


Figure 7. Non-dimensional vorticity for the blockage ratio of (a) 9.8% e (b) 19.7% with uncertainties of 29% and 37%, respectively.

We can see in the figure 7 that the vorticity is more concentrated at the separation point ( $\frac{y}{d} = 0.5$ ) and spreads out as it approaches from the mean vortex core position. It is also possible to note that the dead water region vorticity, near the separation points, seems to be of opposite signal that contained in the shear layer. Due to high uncertainties presented in these results is not possible to affirm anything about the variations suffered by the vorticity field, when the blockage ratio is increased.

The mean vortex core and the saddle points comes into the base direction making the base pressure coefficient more negative, passing from -0.94 to -1.32. We should say here that in this work the base pressure coefficient ( $C_{pb}$ ) is not measured directly, but calculated by the equation (4) (Fage and Johansen, 1927):

$$C_{pb} = 1 - K^2 \quad (4)$$

Where  $K$  is the base pressure parameter and it is defined as the ratio of separation velocity ( $U_s$ ), obtained from the velocity profile through the shear layer, and undisturbed velocity ( $U_\infty$ ).

From the figure 8 to 11 the points indicated by A and B are the maximum longitudinal fluctuating velocity ( $u_{RMS}/U_\infty$ ) and, C and D, the maximum transversal fluctuating velocity ( $v_{RMS}/U_\infty$ ) positions. The points A and B represent the most used definition for the formation region length, according to Bearman (1965). However these points are smooth peaks and the points around them are inside the uncertainty, letting the real uncertainty of 0.1 for the maximum positions of  $u_{RMS}/U_\infty (X_{ur}/d)$  and  $v_{RMS}/U_\infty (X_{vr}/d)$ . This fact was observed from the velocity profiles around the maximum points.

In the figures 8 and 9 are shown the non-dimensional longitudinal ( $u/U_\infty$ ) and transversal ( $v/U_\infty$ ) mean velocities field, respectively. In both cases we can observe the maximum velocity increment with the blockage ratio increase. This can be associated to the mean vortex strength ( $\Gamma$ ) increasing, that can be defined by equation (5) in its non-dimensional form, from 5.28 at the blockage ratio of 9.8% to 5.98 at greater blockage.

$$\frac{\Gamma}{U_\infty d} = \frac{K^2}{2St} \tag{5}$$

Where  $St$  is the Strouhal number.

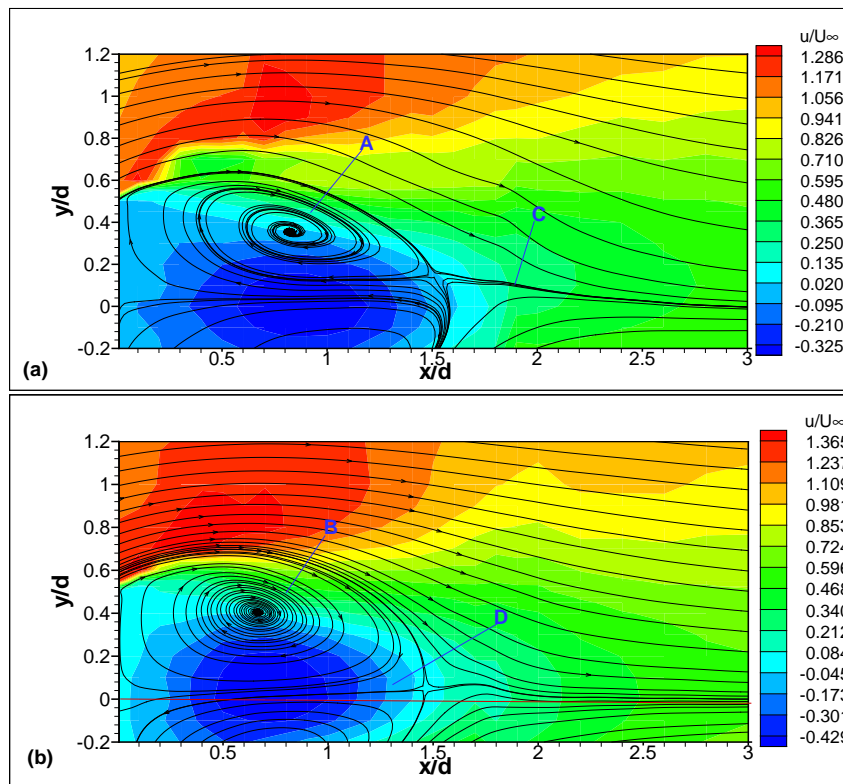


Figure 8. Longitudinal velocity ( $u$ ) field with stream lines for the blockage ratios of (a) 9.8% (non-dimensional uncertainty of  $\pm 0.003$ ) and (b) 19.7% (non-dimensional uncertainty of  $\pm 0.004$ ).

We can also observe in these figures the near wake topology variation due to the blockage ratio increase. The mean vortex core moves forward the body base, decreasing its  $x$ -position ( $X_N/d$ ) from 0.83 to 0.67, and moves away from the symmetry flow line, increasing its  $y$ -position ( $y = 0$ ), from 0.35 to 0.41. The movement in the  $y$ -direction can be explained by the mean vortex growing, which makes the recirculation area becomes larger, what can be confirmed by the increasing in the Strouhal number from 0.184 to 0.194, once this number is associated to vortex formation time. The movement in the  $x$ -direction can be associated to increasing velocity at separation point, which makes the base pressure more negative.

In the figures 10 and 11 are presented the non-dimensional longitudinal ( $u_{RMS}/U_\infty$ ) and transversal ( $v_{RMS}/U_\infty$ ) fluctuant velocities, respectively. As in the case of mean velocities, we can see a small increase in their maximum with the blockage increment. This can be explained by the vortex strength increasing, what increases each vortex induced velocities. It is visible from these figures, where the maximum positions get closer the base body as could be observed for mean vortex core  $x$ -position, presenting a good correlation with it.

In the table 1 are presented the flow parameters variation summary for both blockage ratios. This table shows that there exist good agreements among all the flow parameters. As we can see the blockage ratio increasing leads to the

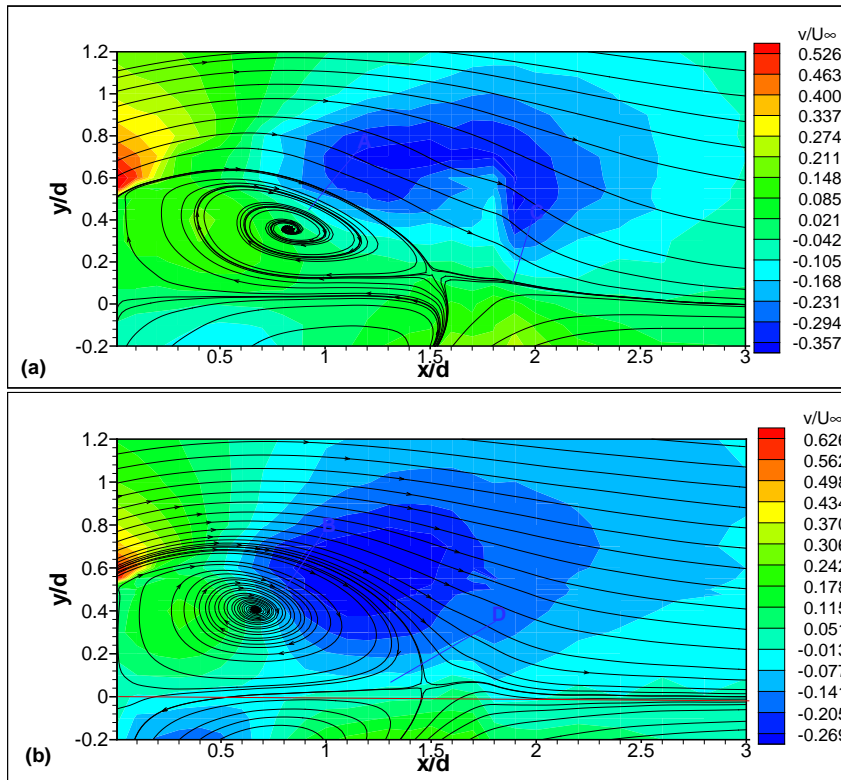


Figure 9. Transversal velocity ( $v$ ) field with stream lines for the blockage ratios of (a) 9.8% (non-dimensional uncertainty of  $\pm 0.004$ ) and (b) 19.7% (non-dimensional uncertainty of  $\pm 0.005$ ).

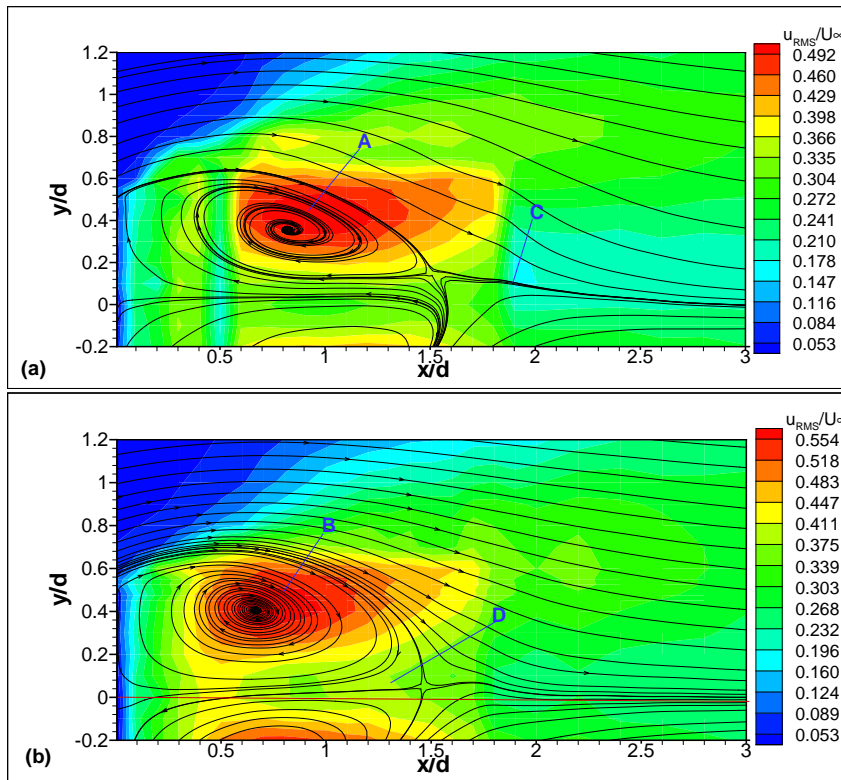


Figure 10. Longitudinal fluctuant velocity field with stream lines for the blockage ratios of (a) 9.8% (non-dimensional uncertainty of  $\pm 0.002$ ) and (b) 19.7% (non-dimensional uncertainty of  $\pm 0.003$ ).

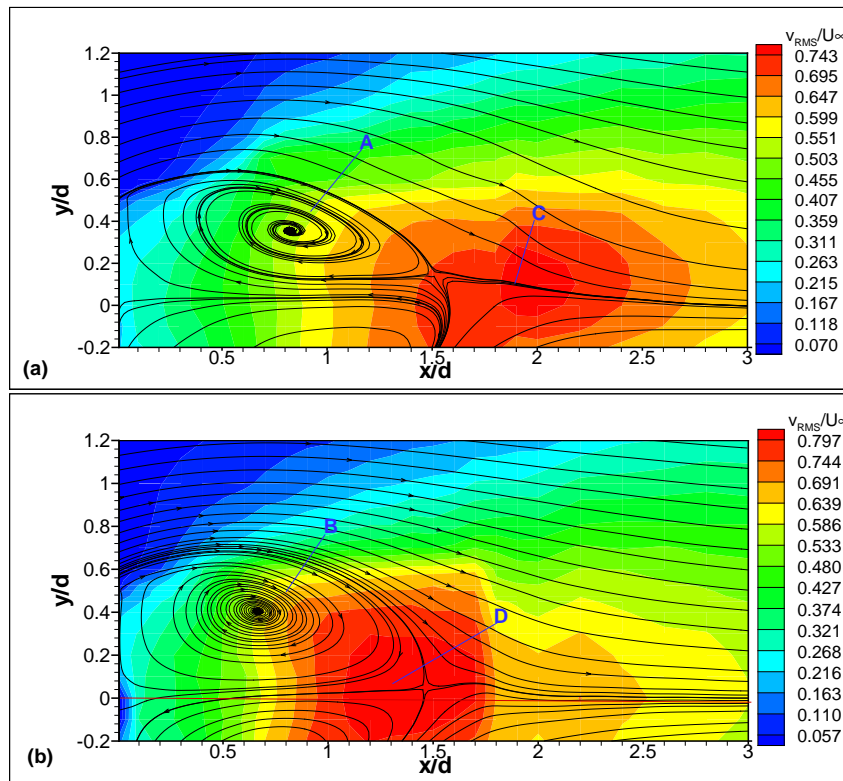


Figure 11. Transversal fluctuant velocity field with stream lines for the blockage ratios of (a) 9.8% (non-dimensional uncertainty of  $\pm 0.002$ ) and (b) 19.7% (non-dimensional uncertainty of  $\pm 0.003$ ).

decrement in the x-positions of the mean vortex core and of maximum longitudinal and transversal fluctuant velocities, while the other parameters are incremented by the blockage ratio increasing.

Table 1. Flow parameters variation due to blockage ratio increasing for 45° wedge.

Blockage	$\frac{X_N}{d}$	$\frac{Y_N}{d}$	$\frac{X_{ur}}{d}$	$\frac{Y_{ur}}{d}$	$\frac{X_{vr}}{d}$	$K$	$C_{Pb}$	St	$\frac{\Gamma}{U_\infty d}$
9,8%	0,83	0,35	0,9	0,4	1,9	1,394	-0,94	0,184	5,28
19,7%	0,67	0,41	0,7	0,4	1,3	1,523	-1,32	0,194	5,98

Due to results absence at the same Reynolds number and blockage ratio the results presented in this section we have not compared the present results with obtained by other authors. However, Roshko (1954) has obtained results for a 90° wedge at the Reynolds number of  $3.9 \times 10^3$  and blockage ratio close (6.1%) to this work, obtaining Strouhal number equal of 0.179, base pressure parameter equal to 1.395 and  $C_{pb}$  of -0.95. These shows good agreement to the results presented here.

Sousa (1993) also made experimental studies with blockage ratio variation, but the Reynolds number in his work was much higher ( $2.8 \times 10^4$  and  $6.5 \times 10^4$ ) using blockage ratios of 7.9% and 18.8%. Although the results are not presented here, his results have the same tendency of the present work.

### 5. Final Remarks

The measurements in near wake flow represented a difficult for such a Reynolds number due to associated calibration uncertainty, mainly for the intrusive method used so far, hot wire anemometry. From the results presented here we can see that laser Doppler anemometry fits well to the task.

Other problem faced in this work was the lack of experimental data about such a wedge model at low Reynolds number, then this work presents new interesting results, such as fluctuant velocities fields and experimental vorticity field, which can be used for DNS validation.

With exception of vorticity field that had large uncertainty due to position measurements associated to the traverse

system, the results presented in this work have good accuracy reflecting the used experimental procedure suitability. These results also presented a good correlations among them for the blockage ratio presented, however more variation is needed for better conclusions.

The measurements also presented, within the possible, good agreement to Roshko (1954) results, which have slightly different Reynolds number, and present the same tendency obtained by Sousa (1993).

## 6. Acknowledgements

To the Coordenação de Aperfeiçoamento de Pessoal de Nível Superior (CAPES) and to the Fundação Casimiro Montenegro Filho, for supporting part of the resources used in this research. To all the staff of the Prof. K.L. Feng Aeronautical Engineering Laboratory. To FAPESP and EMBRAER for the financial support used to acquire the LDA equipment.

## 7. References

- Ahlborn, B.; Seto, M.L.; Noack, B.R., 2002, "On drag, strouhal number and vortex street structure" *Fluid Dynamics Research*, vol. 30, pp 379-399.
- Araújo, T.B., 2008, "Influência do ângulo de separação na esteira próxima de escoamentos bidimensionais sobre corpos rombudos", Msc Thesis - Instituto Tecnológico de Aeronáutica.
- Araújo, T.B. and Girardi, R.M., 2008, "Laser Doppler anemometry application for wedges near wake study", *Proceedings of 12th Brazilian Congress of Thermal Engineering and Sciences*, vol. 1, Belo Horizonte, Brazil.
- Araújo, T.B. and Girardi, R.M., 2009, "Separation Angle Influence in the Near Wake of 2-D Bluff Body", *Proceedings of 20th International Congress of Mechanical Engineering*, Gramado, Brazil.
- Bearman, P.W., 1965, "Investigation of flow behind a two-dimensional model with a blunt trailing edge and fitted with splitter plates", *Journal of Fluid Mechanics*, Vol.21, pp. 241-255.
- Dantec Dynamics, 2005, "BSA flow software version 4 instalation and user's guide".
- Page, A. and Johansen, F.C., 1927, "On the flow of air behind an inclined flat plate of infinite span", *Proc. Roy. Soc.*, vol. 116, pp.170-197.
- Melling, A., 1997, "Tracer particles and seeding for particle image velocimetry", *Meas. Sci. Technol.* Vol.8, pp.1406-1416
- Mittal, S., 2001, "Computation of three-dimensional flow past circular cylinder of low aspect ratio", *Physics of Fluids*, Vol.13, pp. 177-191.
- Rathakrishnan, E., 1999, "Effect os splitter plate on bluff body drag", *AIAA Journal Technical Report*.
- Roshko, A., 1954, "On the Drag and Shedding Frequency of Two-dimensinal Bluff Bodies", *NACA Technical Note 3169*.
- Sousa, F.L., 1993, "Influência da razão de bloqueio no escoamento plano sobre corpos rombudos", Msc Thesis - Instituto Tecnológico de Aeronáutica.
- Tamura, Y.; Kikuchi, H.; Hibi, K., 2003, "Quasi-static wind load combinations for low and middle-rise buildings", *Journal of Wind Engineering and Industrial Aerodynamics*, vol 91, pp. 13.
- Williamson, C. H. K., 1996, "Vortex Dynamics in the Cylinder Wake", *Annual Reviews of Fluid Mechanics*, Vol.28, pp. 477-539.

## 8. Responsibility notice

The author(s) is (are) the only responsible for the printed material included in this paper